

Layered $\text{Li}_x\text{Mn}_{1-y}\text{Co}_y\text{O}_2$ Intercalation Electrodes—Influence of Ion Exchange on Capacity and Structure upon Cycling

Alastair D. Robertson, A. Robert Armstrong, and Peter G. Bruce*

School of Chemistry, University of St. Andrews, St. Andrews, Fife KY16 9ST, Scotland, UK

Received December 11, 2000. Revised Manuscript Received April 3, 2001

Layered $\text{Li}_x\text{Mn}_{1-y}\text{Co}_y\text{O}_2$ with the O3 (αNaFeO_2) structure has been prepared from the analogous P3 sodium phase by ion exchange using LiBr in either ethanol at 80 °C or hexanol at 160 °C. The former preserves, to some extent, vacancies present on the transitional metal sites of the sodium phase, whereas the latter eliminates the vacancies. Materials with vacancies exhibit better performance as cathodes in rechargeable lithium batteries. The 2.5% Co doped material prepared in ethanol exhibits capacities of 200 mAhg^{-1} when cycled at C/8 between 2.4 and 4.6 V at 30 °C and with a fade of only 0.08% per cycle. A capacity of 180 mA h g^{-1} can be obtained at C/2 and 200 mAhg^{-1} at C rate and 55 °C. Importantly, this performance is obtained despite the fact that the materials convert to spinel-like phases on cycling. The spinel-like phases that form are nanostructured, with each crystallite being composed of a mosaic of nanodomains. The relief of strain at the domain wall boundaries accompanying the cubic-tetragonal phase transition may explain, at least in part, the facile cycling of these materials over a wide composition range (including the 3 V plateau) compared with high-temperature spinel which does not possess such nanodomains. Furthermore, vacancies present in the ethanol materials appear to migrate to the domain walls on cycling, rendering even more facile the Jahn–Teller-driven phase transformation on cycling these materials compared with those prepared in hexanol.

I. Introduction

The search for a lithium intercalation compound capable of replacing LiCoO_2 as the cathode in lithium ion cells represents a key materials challenge.^{1,2} Lithium manganese oxides offer the prospect of lower toxicity and cost as well as increased safety compared with LiCoO_2 . The family of spinels based on $\text{Li}_{1+x}\text{Mn}_{2-x}\text{O}_4$ has been investigated extensively and capacities of 120 mAhg^{-1} may be obtained on cycling in the region of 4 V.^{3–6} However, higher capacities are desirable since LiCoO_2 can already deliver 130–140 mAhg^{-1} .

Since the first reports of layered LiMnO_2 , interest in such materials as intercalation electrodes has grown rapidly.^{7–10} It has been shown previously that doping layered LiMnO_2 improves its performance, including capacity and its retention.^{11,12} To this end Mn has been substituted in part by a variety of other ions including

Al, Ni, Co, and Cr.^{11–15} All such compounds are structurally analogous to the O3 structure of conventional LiCoO_2 and consist of cubic close-packed oxide ions with alternate sheets of the octahedral sites between oxide ion layers being occupied by Li and the transition metal ions. Other layered structures are possible, including the O2 structure in which the oxide ions are stacked in an ACAB sequence instead of the ABC stacking of O3. Layered compounds with the O2 structure have been investigated most recently and most extensively by Paulsen and Dahn.^{17,18}

Co-doped LiMnO_2 with the O3 structure has been prepared from the layered P3 Na analogue, $\text{Na}_x\text{Mn}_{1-y}\text{Co}_y\text{O}_2$, by ion exchange in a solution of LiBr in hexanol at 160 °C.^{11,14,15} Recently, we have shown that ion exchange in hexanol at 160 °C results not only in the exchange of Na by Li but in addition to the alteration of the transition metal oxide subarray, whereas exchange under milder conditions, such as 80 °C in ethanol, does not. The ion exchange synthesis in hexanol and ethanol,

* To whom correspondence should be addressed.

(1) Bruce, P. G. *J. Chem. Soc. Chem. Commun.* **1997**, 1997, 1817 and references therein.

(2) Koksang, R.; Barker, J.; Shi, H.; Saiidi, M. Y. *Solid State Ionics* **1996**, *84*, 1 and references therein.

(3) Thackeray, M. M.; David, W. I. F.; Bruce, P. G.; Goodenough, J. B. *Mater. Res. Bull.* **1983**, *18*, 461.

(4) Gummow, R. J.; De Kock, A.; Thackeray, M. M. *Solid State Ionics* **1994**, *69*, 59.

(5) Tarascon, J. M.; McKinnon, W. R.; Coowar, F.; Bowmer, T. N.; Amatucci, G.; Guyomard, D. *J. Electrochem. Soc.* **1994**, *141*, 1421.

(6) Gao, Y.; Dahn, J. R. *J. Electrochem. Soc.* **1996**, *143*, 100.

(7) Armstrong, A. R.; Bruce, P. G. *Nature* **1996**, *381*, 499.

(8) Capitaine, F.; Gravereau, P.; Delmas, C. *Solid State Ionics* **1996**, *89*, 197.

(9) Vitins, G.; West, K. *J. Electrochem. Soc.* **1997**, *144*, 2587.

(10) Tabuchi, M.; Ado, K.; Kobayashi, H.; Kageyama, H.; Masquelier, C.; Kondo, A.; Kanno, R. *J. Electrochem. Soc.* **1998**, *145*, L149.

(11) Armstrong, A. R.; Gitzendanner, R.; Robertson, A. D.; Bruce, P. G. *J. Chem. Soc. Chem. Commun.* **1998**, 1998, 1833–1834.

(12) Jang, Y.-I.; Huang, B.; Y.-M. Chiang, D. Sadoway, R. *Electrochem. Solid State Lett.* **1998**, *1*, 13.

(13) Dahn, J. R.; Zheng, T.; Thomas, C. L. *J. Electrochem. Soc.* **1998**, *145*, 851.

(14) Armstrong, A. R.; Robertson, A. D.; Gitzendanner, R.; Bruce, P. G. *J. Solid State Chem.* **1999**, *145*, 549.

(15) Armstrong, A. R.; Robertson, A. D.; Bruce, P. G. *Electrochim. Acta* **1999**, *45*, 285.

(16) Mishra, S. K.; Ceder, G. *Electrochem. Solid State Lett.* **1999**, *2*, 550.

(17) Paulsen, J. M.; Dahn, J. R. *Solid State Ionics* **1999**, *126*, 3.

(18) Paulsen, J. M.; Dahn, J. R. *J. Electrochem. Soc.* **1999**, *146*, 3560.

along with the influence that changing the synthesis conditions has on the structure and composition of the resulting lithium compounds, has been reported previously.^{19,20} In the present paper we explore how the differences in composition and defect chemistry of the host, induced by differences in the ion exchange conditions, influence aspects of the electrochemistry and structure.

II. Experimental Section

A more detailed description of the synthesis procedure is given in ref 20. $\text{Na}_x\text{Mn}_{1-y}\text{Co}_y\text{O}_2$ compounds were prepared by mixing Na_2CO_3 (Aldrich, 99.5+%), $\text{Mn}(\text{CH}_3\text{CO}_2)_2 \cdot 4\text{H}_2\text{O}$ (Aldrich, 99+%), and $\text{Co}(\text{CH}_3\text{CO}_2)_2 \cdot 4\text{H}_2\text{O}$ (Aldrich, 98+%) in distilled water. The mixture was subjected to rotary evaporation at 80 °C and then heating at 250 °C for 12 h, followed by 630–720 °C for 1 h. Ion exchange was carried out using LiBr as the lithium source and involved refluxing a 7–8-fold excess of this salt with the appropriate Na phase in either ethanol at 80 °C or hexanol at 160 °C.

Chemical analysis for Na and Li was conducted with flame emission and for Mn and Co with atomic absorption spectroscopy. Average transition metal oxidation states were determined by redox titration using ferrous ammonium sulfate/ KMnO_4 . Powder X-ray diffraction data were collected on a Stoe STADI/P diffractometer operating in the transmission mode and utilizing an Fe $\text{K}\alpha_1$ source ($\lambda = 1.936 \text{ \AA}$) to avoid the problem of fluorescence encountered when using a Cu source with manganese-rich compounds. A small angle position sensitive detector was used to collect the data. Surface area measurements were carried out using the BET method employing a Micromeritics Gemini 23670 instrument and yielded values of 5–10 $\text{m}^2 \text{ g}^{-1}$ for samples prepared in ethanol and hexanol. The electrochemical performance of the layered materials was evaluated by constructing composite positive electrodes using a mixture of the active material, Kynar Flex 2801 (a copolymer based on PVDF), and carbon in the weight ratios 85:5:10. The mixture was prepared as a slurry in THF and spread onto aluminum foil using a Doctor Blade technique. Following evaporation of the solvent and drying, electrodes were incorporated into an electrochemical cell in which the second electrode was lithium metal and the electrolyte was a 1 molal solution of LiPF_6 [Hashimoto] in either propylene carbonate or a mixture of ethylene carbonate/diethyl carbonate (Merck) in the volume ratio 1:2. All electrochemical measurements were carried out using a Biologic MacPile II, and the cells were located in a thermostatically controlled chamber maintained at either 30 or 55 ± 0.5 °C. All reported measurements were at 30 °C, unless otherwise stated. After cycling, selected cells were transferred to an argon-filled glovebox and disassembled, and the cathode material was removed. Ex situ X-ray diffraction was then performed on the cathode sample, and the lattice parameters were determined using the GSAS program package.²¹

III. Results and Discussion

Exchange in Ethanol vs Hexanol. Samples of layered P3 sodium manganese oxides with various levels of Co doping were prepared. For each doping level the material was divided into two portions, one was ion exchanged in ethanol at 80 °C and the other in hexanol at 160 °C, as described in the Experimental Section. Cells were constructed and the variation of discharge

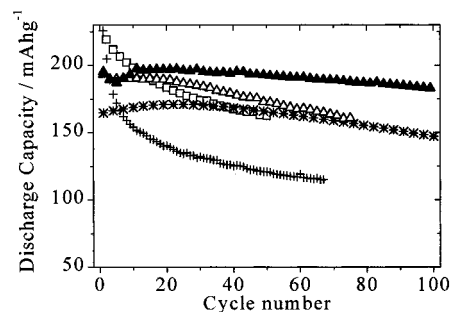


Figure 1. Discharge capacity as a function of cycle number for layered $\text{Li}_x\text{Mn}_{1-y}\text{Co}_y\text{O}_2$: \square , 10% Co prepared in hexanol; $*$, 10% Co prepared in ethanol; \triangle , 2.5% Co prepared in ethanol; \blacktriangle , 2.5% Co prepared in ethanol; and $+$, $\text{LiMn}_{1.95}\text{Co}_{0.05}\text{O}_4$ spinel prepared by high-temperature solid-state reaction. Rate = 25 mA g^{-1} , potential range 2.4–4.6 V.

capacity with cycle number for Co doping levels of 2.5 and 10% are presented in Figure 1. Although the 10% Co doping samples refluxed in hexanol exhibit a high initial capacity, this falls to a value that is comparable to the same 10% Co doping compound prepared in ethanol. Reducing the Co content to 2.5% increases the capacity retention. Increasing the Co content beyond 10% reduces the capacity (see later and ref 14). A high initial capacity that then fades substantially is of little use in the context of rechargeable lithium batteries; hence, capacity retention is a key property in designing materials in this field. The sample with 2.5% Co prepared in ethanol possesses the best combination of initial capacity and capacity retention of any sample, whether prepared in ethanol or hexanol, up to 30% Co doping.

It is evident from the above results that the ion exchange conditions do not simply induce the exchange of Na by Li but changes the material in other ways that affect the cycling performance. As shown in a previous paper, all lithium samples, regardless of Co content or ion exchange conditions, adopt a trigonal layered structure in space group $R\bar{3}m$. However, the a and c lattice parameters are respectively smaller and larger in the case of the ethanol samples when compared with those prepared in hexanol with the same Co content.²⁰ This further emphasizes that the materials prepared using different ion exchange conditions are not identical.

Chemical analysis also reveals important differences (Table 1). The first thing to note is that the parent Na phase is nonstoichiometric; it is deficient in Na, despite the reaction mixture containing one Na per Mn (the excess Na is in the form of Na_2CO_3 , which is removed by washing after exchange).²⁰ More importantly, there are vacancies on the transition metal sites. On refluxing in ethanol at 80 °C these vacancies persist. The vacant sites (in the language of defect chemistry introduced by Kroger–Vink²²), bear a negative effective charge in that region of the crystal structure. This in turn can trap Na^+ ions, resulting in a small amount of residual Na after exchange (Table 1). On the other hand, refluxing in hexanol changes the stoichiometry and defect structure of the transition metal oxide framework, eliminating the vacancies, hence removing Na^+ traps and permitting more complete exchange. We have shown

(19) Robertson, A. D.; Armstrong, A. R.; Bruce, P. G. *J. C. S. Chem. Commun.* **2000**, 2000, 1997.

(20) Robertson, A. D.; Armstrong, A. R.; Fowkes, A. J.; Bruce, P. G. *J. Mater. Chem.* **2001**, *11*, 113.

(21) Larson, A. C.; Von Dreele, R. B. Los Alamos National Laboratory Report Number LA-UR-86-748, 1987.

(22) Tilley, R. J. D. in *Defect Crystal Chemistry and its Applications*, Blackie: London, 1984; p 90.

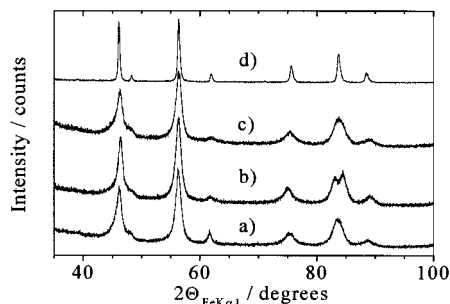


Figure 2. Powder X-ray diffraction patterns for 10% Co-doped materials: (a) prepared in hexanol and after 15 cycles, (b) prepared in ethanol and after 15 cycles, (c) prepared in ethanol and after 50 cycles, (d) stoichiometric $\text{LiMn}_{1.8}\text{Co}_{0.2}\text{O}_4$ spinel prepared by conventional solid-state reaction. Data reported in parts a to c were collected after cycling at 25 mA g^{-1} .

that the differences in the defect chemistry between samples prepared in hexanol and ethanol can explain the differences in the lattice parameters,²⁰ and it is likely that the variation in cycling performance has a similar origin.

The layered lithium manganese oxides doped with cobalt convert to spinel-like phases on cycling, whether the ion exchange process is carried out in hexanol or ethanol; however, the rate of conversion differs, depending on the ion exchange conditions. Powder X-ray diffraction patterns collected after cycling the 10% Co-doped materials prepared in hexanol at 160°C and ethanol at 80°C are presented in Figure 2. Note cycling is stopped at 3.5 V, at which point the samples are single phase. In the case of the compound prepared in ethanol, the structure remains layered after 15 cycles, as is evident from the presence of the 108 and 110 peaks at 83.16° and 84.45° in 2θ , respectively ($\text{Fe K}\alpha_1$). In contrast, the compound prepared in hexanol already shows spinel-like characteristics, the 108 and 110 peaks having merged into a broad peak as the c/a ratio approaches 4.9. A c/a of 4.9 would correspond to a cubic unit cell. On more extended cycling, the compound prepared in ethanol also converts to a spinel-like phase (Figure 2c). In general, the samples synthesized in ethanol convert more slowly on cycling than do the compounds prepared in hexanol. The fact that the lattice parameters of the materials obtained after cycling, for ethanol and hexanol, are very similar is interesting and suggests that vacancies are no longer present in the bulk ethanol sample after cycling. We shall return to this point later in the paper.

Performance of the Materials Prepared in Ethanol. Data on the electrochemical performance of materi-

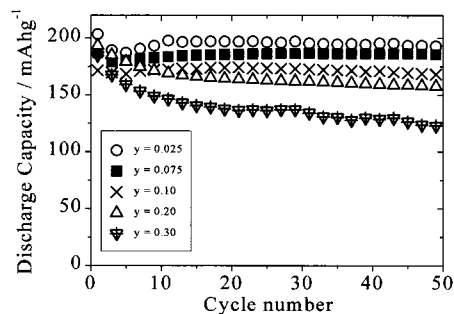


Figure 3. Discharge capacity as a function of cycle number for layered $\text{Li}_x\text{Mn}_{1-y}\text{Co}_y\text{O}_2$ materials prepared in ethanol with different Co contents. Rate = 25 mA g^{-1} , potential range 2.4–4.6 V.

als prepared in hexanol have been presented before.^{11,14,15} Here we focus on the compounds prepared in ethanol. A comparison of the discharge capacity as a function of the cycle number for materials prepared in ethanol but with different Co contents is shown in Figure 3. The initial discharge capacities for all compositions, when the compounds are still layered, are very similar. This is not the case after a number of cycles, when the compounds have converted to the spinel-like phases. A clear trend emerges in which the 2.5% Co-doped samples exhibit the highest capacity, and this capacity decreases with increasing Co content. High-temperature lithium manganese oxide spinel doped with cobalt, $\text{LiMn}_{2-y}\text{Co}_y\text{O}_4$, has been studied, and it is known that in order to access the $\text{Co}^{4+/3+}$ couple, potentials in the region of 5 V are required because the lithium ions are in tetrahedral, 8a sites. Since the high-voltage cutoff used in the present work is limited to 4.6 V, it is unlikely that the $\text{Li}_{8a}\text{-Co}^{4+/3+}$ redox couple is active, electrochemical activity being confined to the $\text{Mn}^{4+/3+}$ couple. The maximum capacity possible if the electrochemistry is limited to this manganese couple, will decrease as the Co content increases. If we take for example the 30% Co-substituted materials, then the theoretical capacity based on accessing only the $\text{Mn}^{4+/3+}$ couple is 197.4 mAh g^{-1} , which is substantially lower than the theoretical capacity for the undoped material, 285.5 mAh g^{-1} . Although the practical capacities reported in Figure 3 do decrease in line with the reduction in the theoretical capacity based on the manganese couple, it should still be noted that the practical capacity for the compound doped with 30% Co is only 130 mAh g^{-1} , which is significantly less than the theoretical value based on Mn alone.

The influence of Co content on the conversion from the layered to spinel-like structure for the materials

Table 1. Compositions of Materials, Prepared by Ion Exchange in Ethanol at 80°C and Hexanol at 160°C

nominal Co content	composition	av TM oxidation state	% TM vacancies	% Mn^{3+} occupancy of TM sites
0.025	$\text{Na}_{0.518}\text{Mn}_{0.908}\text{Co}_{0.025}\text{O}_2$	(a) Na phase 3.731+	67	22.6
0.025	$\text{Na}_{0.051}\text{Li}_{0.564}\text{Mn}_{0.893}\text{Co}_{0.025}\text{O}_2$	(b) Ethanol, 80°C 3.687+	8.2	26.4
0.05	$\text{Na}_{0.032}\text{Li}_{0.604}\text{Mn}_{0.878}\text{Co}_{0.051}\text{O}_2$	3.621+	7.1	30.1
0.10	$\text{Na}_{0.035}\text{Li}_{0.539}\text{Mn}_{0.870}\text{Co}_{0.087}\text{O}_2$	3.580+	4.3	31.5
0.30	$\text{Na}_{0.019}\text{Li}_{0.593}\text{Mn}_{0.657}\text{Co}_{0.297}\text{O}_2$	3.551+	4.6	13.1
0.025	$\text{Na}_{0.009}\text{Li}_{0.619}\text{Mn}_{0.960}\text{Co}_{0.028}\text{O}_2$	(c) Hexanol, 160°C 3.413+	1.2	55.0
0.05	$\text{Na}_{0.008}\text{Li}_{0.608}\text{Mn}_{0.949}\text{Co}_{0.053}\text{O}_2$	3.377+	0.0	57.0
0.10	$\text{Na}_{0.012}\text{Li}_{0.642}\text{Mn}_{0.901}\text{Co}_{0.094}\text{O}_2$	3.363+	0.0	54.0
0.30	$\text{Na}_{0.011}\text{Li}_{0.626}\text{Mn}_{0.692}\text{Co}_{0.316}\text{O}_2$	3.336+	0.0	35.3

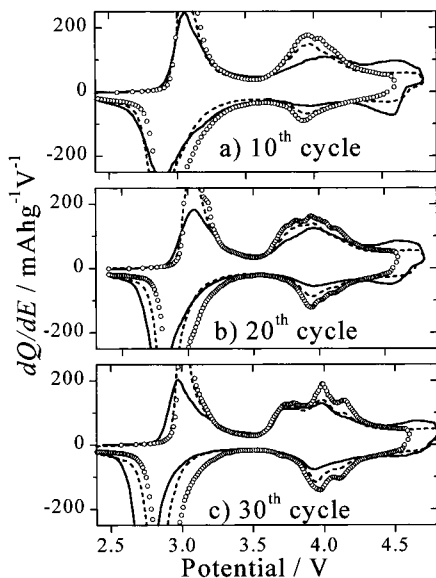


Figure 4. Incremental capacity plots for three different Co contents in layered $\text{Li}_x\text{Mn}_{1-y}\text{Co}_y\text{O}_2$, $y = 0.025$ (\circ), 0.1 (---) and 0.2 (—) and at three different cycle numbers (materials prepared in ethanol).

prepared in ethanol has been probed by determining the incremental capacity plots as a function of cycle number for several Co-doping levels (Figure 4). After 10 cycles, the materials containing 2.5% Co already possess some capacity in the 4 V region. The 4 V capacity is somewhat less in the case of the sample with 10% Co and significantly less for the 20% Co materials. After 20 cycles the 20% Co-doped material shows increased capacity in the 4 V region; however, the double 4 V redox process characteristic of spinel is not yet evident. After 30 cycles and for the lowest Co content of 2.5%, there is clear evidence of the double 4 V process, indicating that spinel-like regions are now well-established in the material. The evidence for spinel-like regions is progressively less for the higher Co-doping levels. The trend toward a less facile transformation with higher Co content is in accord with our previous observations for Co-doped lithium manganese oxide materials prepared in hexanol and is consistent with the fact that the Co-rich end member of this solid solution series, LiCoO_2 , is stable as a layered phase.^{14,15}

An important practical feature of any lithium intercalation cathode for rechargeable lithium batteries is the extent to which capacity decreases on cycling at higher rates. To illustrate the rate capability of the materials prepared in ethanol, discharge capacities at three different rates are presented for the optimum (2.5% Co) material in Figure 5. At the lowest rate of 10 mA g^{-1} , capacities in excess of 200 mAh g^{-1} are sustained on cycling. The transformation to a spinel-like compound on cycling introduces a kinetic barrier within the first 10–30 cycles, as is evident in the slow rise in capacity within the early stages of cycling for the 100 mA g^{-1} rate. The conversion occurs at higher cycle number with increasing rate, rising from between 15 and 25 cycles for the lowest rate of 10 mA g^{-1} to more than 35 cycles for the 100 mA g^{-1} rate, as evidenced by the incremental capacity plots (Figure 6). Once the material has converted to a spinel-like phase, the capacity is influenced much less by the cycling rate. For

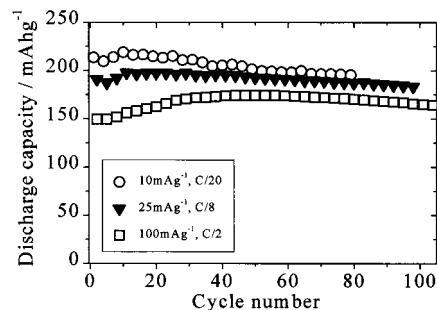


Figure 5. Discharge capacity as a function of cycle number for 2.5% Co-doped layered material at three different rates, 10, 25, and 100 mA g^{-1} between potential limits of 2.4–4.6 V (materials prepared in ethanol).

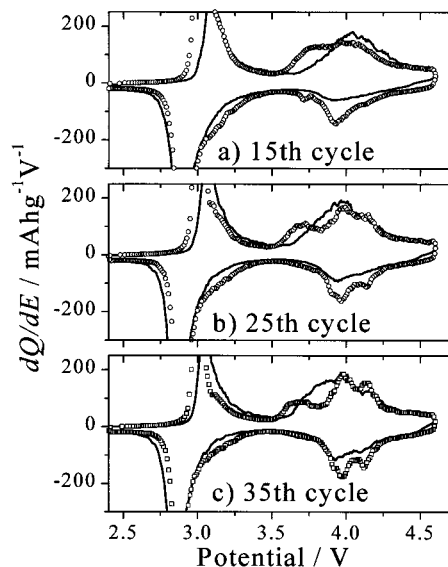


Figure 6. Incremental capacity plots for 2.5% Co-doped layered material at two rates, 10 mA g^{-1} (\circ) and 100 mA g^{-1} (\square) and at three different cycle numbers (materials prepared in ethanol).

example, for the 2.5% Co-doped material, between 40 and 50 cycles the discharge capacity drops by only 10 and 30 mA g^{-1} as the rate is increased respectively from 10 to 25 and 100 mA g^{-1} (Figure 5). It should also be noted that we have not attempted to optimize the construction of the composite cathode in terms of rate capability (e.g., percentage carbon, control of particle size), and therefore, it is likely that the rate performance could be further improved. As well as the absolute discharge capacity, it is instructive to consider at what voltage this capacity is delivered as a function of the state-of-charge and how the voltage curve might be influenced by the cycling rate. In Figure 7 we present the discharge voltage curves for three rates after 30 cycles. The basic shape of the curve is invariant with rate. As the rate is increased, capacity is reduced at 3 and 4 V, although the extent of the reduction is slightly greater at 3 V. It is worth noting that the cobalt-doped materials presented here and prepared by ion exchange exhibit high capacities of around $160\text{--}170 \text{ mAh g}^{-1}$ at high rates, and this appears to be in contrast to similar materials prepared directly by high-temperature solid-state reaction involving other dopants such as aluminum or chromium, where high capacities may be obtained at high rate and elevated temperatures of

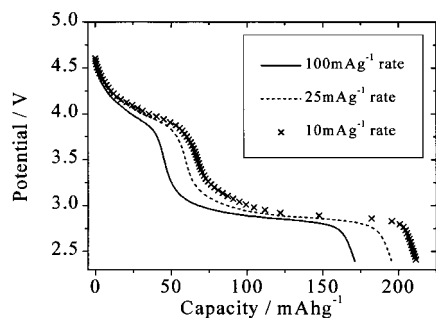


Figure 7. Voltage vs state-of-charge for 2.5% Co-doped layered material prepared in ethanol after 30 cycles and at three different rates.

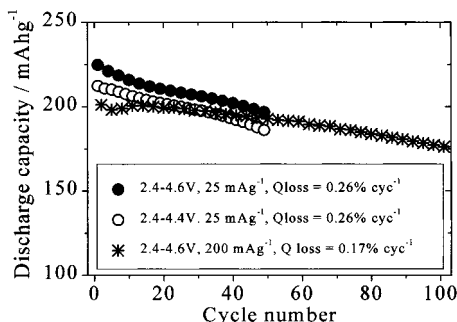


Figure 8. Discharge capacity as a function of cycle number at 55 °C for 2.5% Co-doped layered material prepared in ethanol.

around 55 °C, but rate capability appears typically to be somewhat less at room temperature.^{12,24}

Although at elevated temperatures of around 55 °C high rate capability is easy to achieve, it may also lead to increased capacity fade due to Mn dissolution. It is important to consider high-temperature performance in the context of practical materials. The capacity fades obtained at 55 °C and at rates of 25 and 200 mA g⁻¹ for our optimum material with 2.5% Co-doping prepared in ethanol are shown in Figure 8. It may be noted that the variation of capacity in the first 10–15 cycles observed at 30 °C disappears at higher temperatures, and this reinforces the view that the process is related to the kinetics of the transformation. The capacity fade at 55 °C is somewhat greater (0.26% per cycle) at 55 °C compared with 0.08% at 30 °C when cycled over the same voltage range, 2.4–4.6 V. Reducing the upper voltage limit from 4.6 to 4.4 V does not reduce the fade rate but does result in a slight reduction in the absolute values of the capacity. The fade rate is less at the higher cycling rate of 200 mA g⁻¹. At higher rates the time taken for a given number of cycles is correspondingly reduced so that the time of exposure of the electrode to the electrolyte and hence the degree of dissolution will be less. The incremental capacity plots derived from the 2.4–4.6 V, 25 mA g⁻¹ cycling data at 55 °C are shown for three cycle numbers in Figure 9. It is interesting to note that that the double 4 V process appears within 10 cycles compared with 20 cycles at 30 °C for the same voltage range and rate. This highlights the effect of cycling kinetics on the rate of the phase transformation.

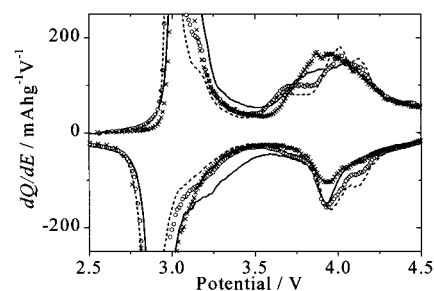


Figure 9. Incremental capacity plots for 2.5% Co-doped ethanol-derived material cycled at 55 °C and 25 mA g⁻¹: —, cycle 5; ○, cycle 10; ---, cycle 15; ×, cycle 15 at 30 °C is shown for comparison.

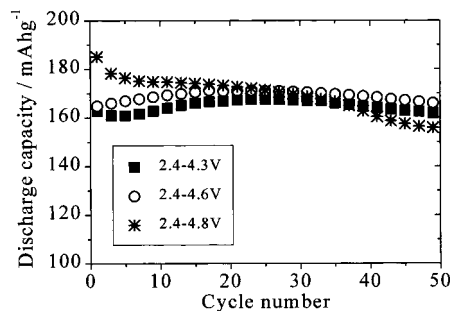


Figure 10. Influence of upper voltage limit on discharge capacity for 10% Co-doped layered material prepared in ethanol and cycled at 25 mA g⁻¹.

To explore in more detail the influence of the high-voltage limit on the capacity fade, the 10% Co-doped material prepared in ethanol was cycled between 2.4 V and three different upper voltage limits, 4.3, 4.6, and 4.8 V. The discharge capacities are shown in Figure 10. The fade rate is unaffected by raising the limit from 4.3 to 4.6 V; however, the fade is greater if the limit is raised still further to 4.8 V. This is probably due to some electrolyte oxidation at this high-voltage cutoff.

Origin of the Differences between Materials Prepared in Hexanol and Ethanol—A Nanostructure Model. There remains the interesting question of why the materials prepared in ethanol should exhibit better capacity retention than those in hexanol. This trend is particularly evident for low Co-doping levels, i.e., less than 20%. Furthermore, the performance of the materials is better at low Co-doping, making such Mn-rich compounds of prime interest. It seems likely that the differences seen at low Co-doping are related to the presence of Na⁺ and transition metal vacancies in the material prepared in ethanol, but why?

It is well-known that LiMn₂O₄ prepared at high temperature, whether stoichiometric or doped with ions such as Li to form Li_{1+x}Mn_{2-x}O₄, exhibits very significant capacity fade when cycled over a wide composition range. (In Figure 1 we present data that shows significant fade for a high-temperature spinel doped with 2.5% Co, and this may be compared directly with the 2.5% Co-doped layered materials.) Cycling over a wide range invariably involves both the 3 and 4 V plateaux and passage through the cubic–tetragonal phase transition. On intercalation of Li beyond the composition LiMn₂O₄ (50% high spin d⁴ Mn³⁺), a tetragonal phase forms at the surface of the crystallites due to the cooperative Jahn–Teller distortion. The tetragonal–cubic phase

(23) Kawai, H.; Nagata, M.; Tukamoto, H.; West, A. R. *Electrochem. Solid State Lett.* **1998**, *1*, 212.

(24) Paulsen, J.; Amundsen, B.; Desilvestro, H.; Steiner, R.; Hassell, D. Abstract 71 of The 198th Electrochemical Society Meeting, Phoenix AZ, October 2000.

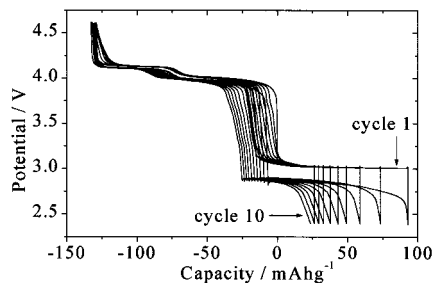


Figure 11. First 10 charge–discharge cycles for $\text{LiMn}_{1.95}\text{Co}_{0.05}\text{O}_4$ spinel prepared by high-temperature solid-state synthesis and cycled over both 3 and 4 V plateaux. Rate = 25 mA g^{-1} .

boundary moves through the particles as intercalation proceeds. Significant strain within the particle must ensue and it might have been expected that this would lead to break up of the particles. If this were so, then capacity would be lost in equal measure from both the 3 and 4 V plateaux on cycling. However, examination of load curves for high-temperature spinel cycled over both plateaux reveals that the fade occurs primarily at 3 V (Figure 11).

The layered Co-doped materials, whether prepared in hexanol or ethanol, convert to spinel-like phases on cycling and also undergo a Jahn–Teller-driven phase transition when cycled over a wide composition range. However, in complete contrast to high-temperature spinel, these materials continue to exhibit a high capacity with minimal fade and certainly retain significant 3 V capacity (Figures 1 and 7). On extraction of Li from layered LiMnO_2 , conversion to a spinel-like phase involves rearrangement of the cations but retention of the cubic close-packed, O3, oxide subarray. We have described previously how the spinel-like phase forms with a nanostructure composed of microdomains within each particle.²⁵ High-resolution electron microscopy reveals directly that the particles are composed of such a nanostructured spinel-like phase (Figure 12a).²⁶ It should be noted that the particles remain intact, and the spinel-like phase is nanostructured but not nanoparticulate. If it was, dissolution in the electrolyte, which is known to occur for manganese oxide based cathodes, would lead to severe capacity losses. Independent evidence for such nanostructuring has been reported recently based on elegant HREM studies that focus in particular on the crystallography associated with the nanostructure especially in Al-doped layered LiMnO_2 and in orthorhombic LiMnO_2 , which also convert to spinel.^{27,28} On cycling such nanostructured materials, the Jahn–Teller-induced phase transition can occur within the particles but with the stress being relieved by slippage at the domain wall boundaries, so that complete domains within a particle can fully transform. The model is illustrated schematically in Figure 12b. In this way facile cycling may occur with

a (111) lattice fringes

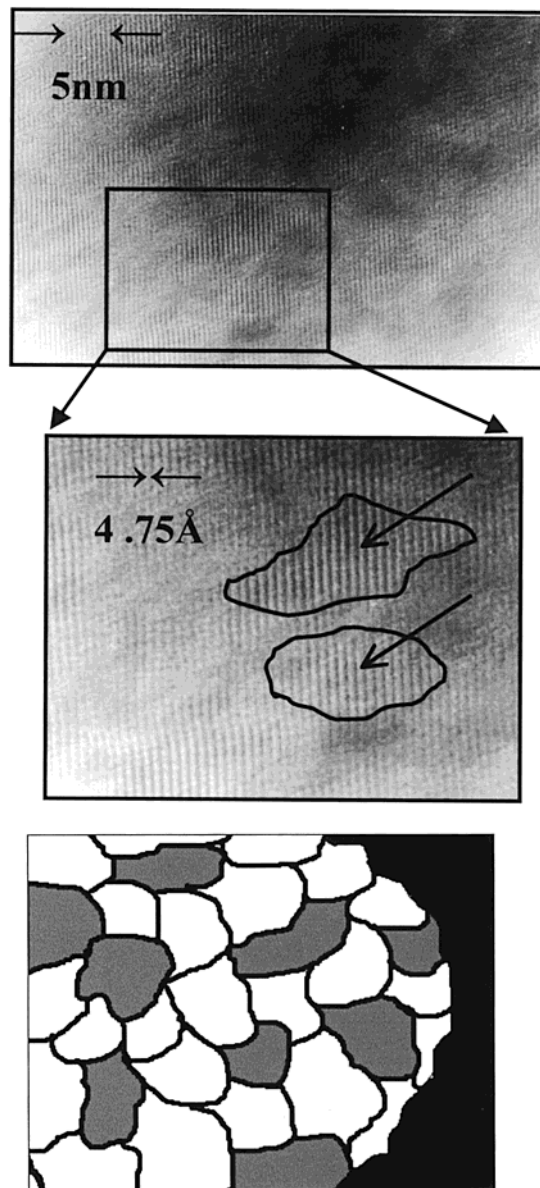


Figure 12. (a) High-resolution transmission electron micrograph indicating the presence of a domain structure in the spinel-like material derived from cycling Co-doped layered LiMnO_2 . (b) Schematic representation of the nanostructured spinel as it converts between cubic and tetragonal phases on cycling. Entire domains switch between the cubic and tetragonal phases with strain being relieved at the domain walls.

minimal capacity loss despite expansion/contraction of the lattice and even despite phase transitions. For the materials discussed in this paper a capacity retention of >99.9 is obtained and of high rates, despite passing through a 1st order Jahn–Teller driven phase transition on each cycle. It is not necessary to strive for zero expansion or to avoid phase transitions in order to ensure facile intercalation and high capacity retention in an intercalation cathode. This strategy is not confined to the manganese materials discussed here. Insertion into other intercalation materials that undergo significant expansion/contraction, or that are associated with phase transitions, could be rendered facile by nanostructuring.

(25) Bruce, P. G.; Armstrong, A. R.; Gitzendanner, R. L. *J. Mater. Chem.* **1999**, *9*, 193.

(26) Shao-Horn, Y.; Hackney, S. A.; Armstrong, A. R.; Bruce, P. G.; Gitzendanner, R.; Johnson, C. S.; Thackeray, M. M. *J. Electrochem. Soc.* **1999**, *146*, 2404.

(27) Wang, H.; Jang, Y. I.; Chiang, Y. M. *Electrochem. Solid State Lett.* **1999**, *2*, 490.

(28) Chiang, Y. M.; Wang, H.; Jang, Y.-I. *Chem. Mater.* **2001**, *13*, 53.

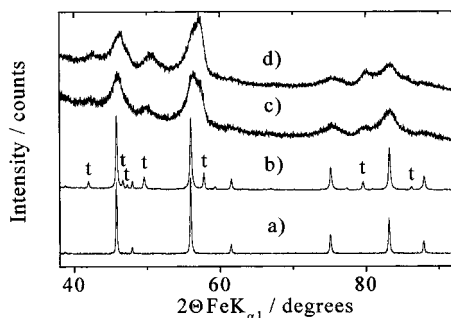


Figure 13. XRD patterns of (a) $\text{LiMn}_{1.95}\text{Co}_{0.05}\text{O}_4$ spinel, prepared by high-temperature solid-state synthesis, (b) $\text{LiMn}_{1.95}\text{Co}_{0.05}\text{O}_4$ spinel after 70 cycles, (c) layered $\text{Li}_x\text{Mn}_{0.975}\text{Co}_{0.025}\text{O}_4$ prepared in hexanol and after 70 cycles, (d) layered $\text{Li}_x\text{Mn}_{0.975}\text{Co}_{0.025}\text{O}_4$ prepared in ethanol and after 70 cycles. All cells stopped at end of discharge, 2.4 V.

Table 2. Composition of Lattice Parameters for Materials Shown in Figure 13

	composition	$a_{\text{cubic}}/\text{\AA}$
(a)	As-prepared high-temperature $\text{LiMn}_{1.95}\text{Co}_{0.05}\text{O}_4$ spinel	8.2452(4)
(b)	High-temperature $\text{LiMn}_{1.95}\text{Co}_{0.05}\text{O}_4$ spinel after 67 complete cycles	8.2454(5)
(c)	$\text{Li}_x\text{Mn}_{1.95}\text{Co}_{0.05}\text{O}_4$ (hexanol 160 °C) undistorted phase (described as cubic) after 70 cycles. $E_{\text{fin}} = 2.4$ V	8.241(1)
(d)	$\text{Li}_x\text{Mn}_{1.95}\text{Co}_{0.05}\text{O}_4$ (ethanol 80 °C) undistorted phase (described as cubic) after 70 cycles. $E_{\text{fin}} = 2.4$ V	8.232(1)

Powder X-ray diffraction patterns for 2.5% Co-doped high-temperature spinel, $\text{LiMn}_{1.95}\text{Co}_{0.05}\text{O}_4$, and 2.5% Co-doped layered materials prepared in hexanol and ethanol are presented in Figure 13. The data are for materials after 70 cycles at 25 mA g^{-1} between 2.4 and 4.6 V. The cells were stopped at the end of discharge. All three cycled materials possess two phases. In the case of the high-temperature material, the phases are cubic and tetragonal spinel. For the hexanol and ethanol materials the peaks are broad, reflecting the nanostructure within the particles; however, they can be ascribed to spinel-like phases that are close to cubic and tetragonal symmetry. The material prepared in ethanol exhibits the greatest proportion of distorted phase, which is consistent with the fact that it exhibits the highest discharge capacity. The high-temperature spinel has the lowest capacity and correspondingly the smallest proportion of tetragonal phase. The lattice parameters of the two undistorted phases derived from the materials prepared in ethanol and hexanol are very similar and are close to the cubic lattice parameter for the undistorted phase obtained from the high-temperature spinel (Table 2). This in turn is close to the value for cubic, stoichiometric, spinel (8.24 Å). Had the vacancies present in the layered material prepared in ethanol been

preserved after conversion to the spinel-like materials, this would not have been the case. It is well-known that defect spinels containing vacancies on the transition metal sites exhibit smaller lattice parameters than stoichiometric LiMn_2O_4 . For example, in the extreme case of $\text{Li}_2\text{Mn}_4\text{O}_9$, the cubic lattice parameter is close to 8.16 Å.²⁹ We propose that the transition metal vacancies present in the ethanol material migrate to the domain walls, rendering the domains stoichiometric and the domain walls more defective than for hexanol samples. Furthermore, we know from EDAX measurements that some Na is still present after 40 cycles in the ethanol samples, even though conversion to a spinel-like phase has occurred after some 25 cycles. Na cannot be in the bulk spinel-like phase but is likely to be present along with the TM vacancies at the domain walls, further facilitating the relief of strain in the ethanol material.

In summary, it is clear that the differences in defect structure and composition between layered $\text{LiMn}_{1-y}\text{Co}_y\text{O}_2$ prepared by ion exchange in ethanol at 80 °C and hexanol at 160 °C have an important influence on the cycling performance, with the ethanol samples, especially at Co-doping levels of less than 10%, exhibiting superior capacity retention. It is necessary to comment on the use of the term spinel-like in this paper to describe the ethanol- and hexanol-derived material after cycling. The layered materials, whether prepared in hexanol or ethanol, exhibit a reduction in the c/a ratios of their hexagonal unit cells as a function of cycle number. In both cases the c/a ratios approach but do not reach a value of 4.9 (which would correspond to a cubic unit cell). Even after extended cycling we observe values for c/a of 4.93 when cycling is arrested at 3.5 V vs Li^+/Li . The powder X-ray diffraction patterns obtained at this voltage approximate closely to a cubic unit cell (see Figures 2 and 13). Because of this and the presence of the double 4 V process, we have referred to the materials after extended cycling as spinel-like. Questions remain concerning the exact nature of the materials obtained on cycling and how similar these are to a spinel structure. We are addressing this issue at present and will return to it in a later paper.

Acknowledgment. P.G.B. is indebted to the EPSRC for financial support. The authors would also like to thank Dr W. Zhou, University of St. Andrews, for help with the HREM measurements.

CM000965H

(29) Thackeray, M. M.; de Kock, A.; Russouw, M. H.; Liles, D.; Bittihn, R.; Hoge, D. *J. Electrochem. Soc.* **1992**, *139*, 363.